PAPER

NJC
www.rsc.org/njc

Growth of $CaCO_3$ in the templated Langmuir–Blodgett film of a bolaamphiphilic diacid

Yi Zhang,[a] Riguang Jin,[a] Li Zhang[b] and Minghua Liu*[b]

[a] *College of Materials Science and Engineering, Beijing University of Chemical Technology, Beijing 100029, China*
[b] *Key Laboratory of Colloid and Interface Science, Institute of Chemistry, Chinese Academy of Sciences, Beijing 10080, China. E-mail: liumh@iccas.ac.cn*

***Received** (in Montpellier, France) 5th November 2003, Accepted 16th January 2004*
First published as an Advance Article on the web 1st April 2004

In this paper, an organic template, the Langmuir–Blodgett (LB) film of a bolaamphiphilic diacid (1,18-octadecanedicarboxylic acid, ODA), was used to grow nanostructured calcium carbonate. ODA can form a stable Langmuir film when it is spread on the aqueous subphase containing $CaCl_2$. FT-IR and XPS spectra of the transferred Langmuir–Blodgett film show that formation of the stable Langmuir film is induced by Ca^{2+} ion. Through immersion of the Ca^{2+} containing LB film of ODA into aqueous Na_2CO_3 solution, nanostructured $CaCO_3$ can be formed in the film. Although nanoparticles were obtained at the initial times, nanorods were obtained after longer growth times. When using a LB film of the calcium salt of stearic acid, only granular particles were found. A possible mechanism is proposed to explain the formation of the nanorods in the templated LB films of these bolaamphiphiles.

Introduction

Inorganic and metal nanoparticles have been intensively studied due to their potential applications in microelectronics[1–3] and for their magnetic, catalytic and optical properties.[4–5] The properties of these inorganic or metal nanomaterials are strongly depended on their size and shape, as well as the interactions between the nanoparticles. Although size control is important for achieving specific properties of materials,[6] shape or morphology control of the nanostructured materials has also proved to be significant.[7–10] For the preparation of inorganic and metal nanostructured materials, template synthesis methods are widely used, which include "soft" templates such as micelles[11] and vesicles[12] and "hard" templates such as Langmuir–Blodgett (LB) films,[13] self-assembled films,[14] nanoporous alumina[15] and carbon nanotubes.[16] Langmuir–Blodgett films are about the most used templates to grow inorganic or metal nanoparticles or nanomaterials.[17–19] However, work on the growth of nanoparticles in LB films of bolaamphiphiles is rare.[20–22]

Bolaamphiphiles are a class of amphiphiles in which two hydrophilic head groups are covalently linked by a hydrophobic alkyl chain.[23–25] Compared with conventional amphiphiles, bolaamphiphiles show abundant interfacial conformations and the potential to form nanostructures in organized assemblies. It has been reported that bolaamphiphiles can form multilayer films or some exotic structures on subphases containing various metal ions.[26–28] As an important biomineral and an industrially useful material, calcium carbonate crystals have been widely studied in the presence of organic templates and/or additives.[29–31] Up to now, the controlled growth of $CaCO_3$ crystals has been studied in templates of ultrathin organic films,[32] self-assembled films[33] and foam lamellae, focusing on control of the polymorph and crystal orientation. In this paper, we have used the LB film of a bolaamphiphilic diacid as a template to investigate the growth and morphology control of calcium carbonate in the film. Some special morphologies were observed, compared with the stearic acid LB film, and possible growth mechanism are discussed.

DOI: 10.1039/b314136e

Experimental

1,18-Octadecanedicarboxylic acid (ODA) was purchased from Tokyo Kasei and was used without further purification. $CaCl_2$, Na_2CO_3 (A.R. grade) were also used without further purification. The subphase was prepared by dissolving $CaCl_2$ in highly purified Millipore Q water (18 MΩ cm) at a concentration of 1×10^{-2} mol L^{-1}. The floating films at the air–water interface were formed by spreading chloroform solutions of ODA (1×10^{-4} mol L^{-1}) on a water surface or subphase containing $CaCl_2$. The surface pressure-molecular area isotherms were measured in a KSV minitrough (KSV 1100, Helsinki, Finland). Thirty minutes after the spread of ODA on the air–aqueous surface, compression of the barrier at a constant speed of 5 mm min^{-1} was performed. The subphase temperature was kept at 20 °C. The Langmuir–Blodgett films were prepared by the vertical dipping method at a constant speed of 5 mm min^{-1} on the KSV trough. $CaCO_3$ nanostructures were formed by simply immersing the Ca(II) containing ultrathin films into the Na_2CO_3 solution (0.1 M, 0.01 M and 0.001 M) for different times at room temperature (*ca.* 20 °C).

The LB films of ODA/Ca(II) were deposited on silicon wafer and CaF_2 substrates for X-ray photoelectron (XPS) spectroscopy and the FESEM observations, Fourier transform infrared (FT-IR) spectra, respectively. The films were washed with water before the FESEM observations. Field emission scanning electron microscopy (FESEM) was performed using a Hitachi S-4300 system. XPS spectra were measured with a VG Scientific ESCALAB 220-IXL spectrometer using Al Kα as the excitation source (1486.6 eV).

Results and discussion

Surface pressure-area isotherms of spreading Langmuir film

Fig. 1 shows the surface pressure-area isotherms of ODA spreading on a pure water surface as well as on the subphase of $CaCl_2$. ODA formed a multilayer Langmuir film or three-dimensional structure on a pure water surface as reported

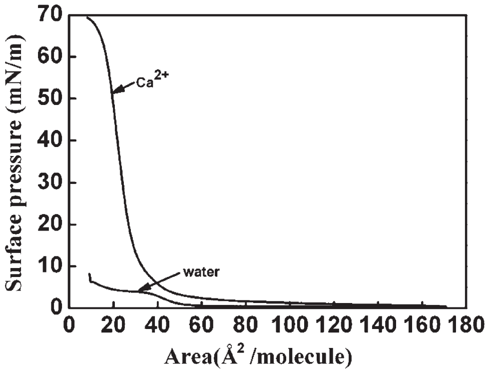

Fig. 1 The surface pressure-area isotherm of ODA spread on a pure water surface and subphase containing Ca(II) ions.

previously.[27] When spreading ODA on the Ca(II) ion subphase, larger changes were observed. The isotherm became condensed and showed a much higher collapse pressure compared with that on pure water. The limiting area was about 30 Å^2 molecule^{-1}. This result strongly indicates some interaction between ODA and Ca^{2+}. Although this value is larger than the cross section of a single chain, it resembles the isotherm in the work of Lahav *et al.* on divalent ions using the GIXD method.[27] So it can be suggested that ODA forms a salt with Ca(II), resulting in a multilayer film.

Characterization of the transferred Langmuir–Blodgett film

To further confirm the metal salt formation of ODA with Ca(II), FT-IR spectra of the LB film transferred from the Ca(II) subphase were compared with the cast film on CaF$_2$ substrates, as shown in Fig. 2. The cast film of ODA shows a strong band at 1698 cm^{-1}, which can be ascribed to the vibrational mode of the hydrogen-bonded carboxylic acid. In the film transferred from the subphase of Ca^{2+}, strong absorption bands were observed at 1570 and 1536 cm^{-1}. These bands were assigned to the asymmetric stretching vibration of carboxylate (COO$^-$), , while a band at 1412 cm^{-1} could be assigned to the symmetric stretching vibration of carboxylate. These spectral changes indicate the salt formation of ODA with Ca^{2+}. In addition, a new band appeared at 1735 cm^{-1} replacing the band at 1698 cm^{-1}, which indicates that upon interacting with Ca^{2+} some of the carboxylic acid groups are liberated.

To further reveal the salt formation in the film, XPS spectra were measured in the transferred film from the water surface and Ca^{2+} ion subphase. In the spectrum of the film transferred from the Ca^{2+} subphase, there appeared a characteristic binding energy of Ca^{2+} at 347.2 eV, indicating the incorporation of Ca^{2+} in the film. Quantitative analysis revealed that the concentration of Ca^{2+} ions was lower than that of ODA. This indicates the incompleteness of the interfacial reaction and is in agreement with the FT-IR spectra.

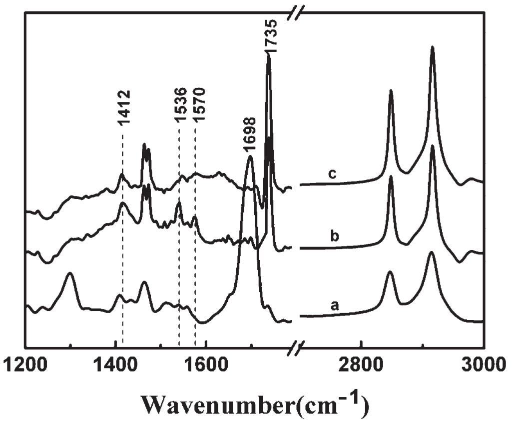

Fig. 2 The FT-IR spectra of (a) ODA cast film, (b) ODA/Ca(II) LB film, (c) ODA/Ca(II) LB film immersed into 0.1 M Na$_2$CO$_3$ for 10 min.

Growth of CaCO$_3$ in the LB film

A Ca^{2+} containing LB film can serve as a template for the formation and growth of CaCO$_3$ nanoparticles. The formation of CaCO$_3$ in the film can be verified by the FT-IR spectra. The two bands ascribed to COO$^-$ and located at 1570 and 1535 cm^{-1} disappeared after immersion into the Na$_2$CO$_3$ solution, while the band at 1735 cm^{-1} increased. This indicates that CaCO$_3$ was formed in the complex film. On the other hand, the absorption peaks at 2920 and 2850 cm^{-1} in the transferred film, which are attributed to the asymmetric and symmetric stretching bands of CH$_2$, did not noticeably change. This means that the conformation of the alkyl chain does not change significantly after formation of CaCO$_3$ in the film.

The morphology of CaCO$_3$ plays an important role in determining the properties of CaCO$_3$. It was observed that various morphologies of CaCO$_3$ could be formed when it is grown in LB films of ODA/Ca^{2+}, as shown by the FESEM images reproduced in Fig. 3. Different concentrations of Na$_2$CO$_3$ were used to investigate the relationship of morphology with the reactant concentration while keeping reaction time constant. Nanoparticles of CaCO$_3$ with a diameter of about 100 nm, shown in Fig. 3(a), were obtained by immersion in 1 mM of Na$_2$CO$_3$ solution. With increasing concentration of Na$_2$CO$_3$, a fern-like morphology, shown in Fig. 3(b), composed of CaCO$_3$ nanorods was observed in the film. At the highest concentration of Na$_2$CO$_3$, nanorods of CaCO$_3$ were obtained in the film [Fig. 3(c)]. These nanorods have a diameter of 100 nm and a length of several hundred nanometers, indicating that they were formed by aggregation of nanoparticles.

In situ formation of nanoparticles by solution reaction methods can be divided into two steps: one is the nucleation of the nanoparticles and the other is the aggregation or diffusion of the nanoparticles in the film. A lower concentration of the reaction solution leads to a slow nucleation speed and further influences the final aggregation morphology. In our case, nanoparticles were observed only in the low concentration Na$_2$CO$_3$ solution. At high concentration, the high rate of nucleation led to the direct aggregation of the CaCO$_3$ nanoparticles into nanorods.

The morphology of the formed CaCO$_3$ was also influenced by the growth time. As shown in Fig. 4, the aggregation morphology changed from nanoparticles to nanorods with increase of the immersion time, even at low Na$_2$CO$_3$ concentration. Globular nanoparticles were found in the film after 2 min of immersion as shown before. Aggregation of the nanoparticles in the film was seen when the immersion time was increased to 5 min. Nanorods of CaCO$_3$ was observed in the film when the immersion time was increased to 600 min. This result indicates that the nanorods are formed by the aggregation of nanoparticles. Upon increasing the concentration of Na$_2$CO$_3$ to 0.1 M, rod-like CaCO$_3$ was observed in the film after the first 2 min of immersion. The diameter of the rods increasing with immersion time (Fig. 5), changing from 100 nm to about 1 μm at the longest immersion times.

We used LB films of stearic acid/Ca^{2+} as a reference and performed similar experiments under similar conditions. Only granular particles were found (Fig. 6) and no nanorod structures of CaCO$_3$ were obtained. Obviously the bola-form amphiphiles play an important role in forming such morphologies.

The formation of the nanorods can be explained by the following mechanism, shown in Scheme 1. It has been reported that ODA can form Langmuir films on a water surface; in these films the alkyl chains are packed parallel to the water

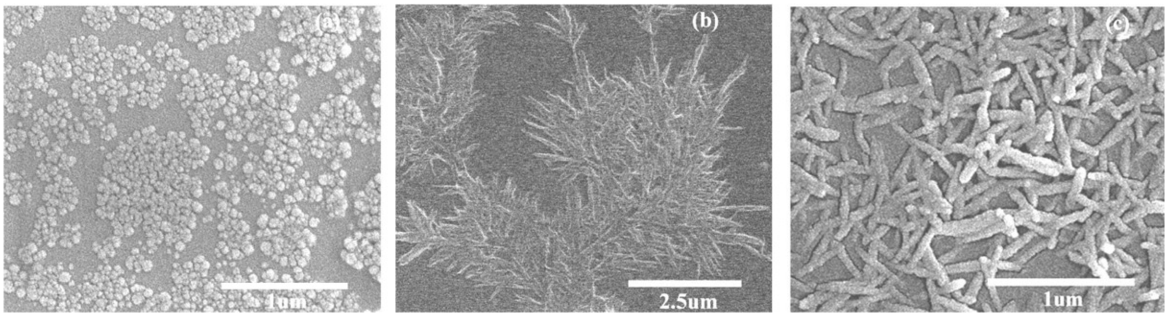

Fig. 3 FESEM images of the morphologies of $CaCO_3$ formed in an ODA/Ca^{2+} LB film after immersing it into (a) 0.001, (b) 0.01, (c) 0.1 M Na_2CO_3 solution for 2 min.

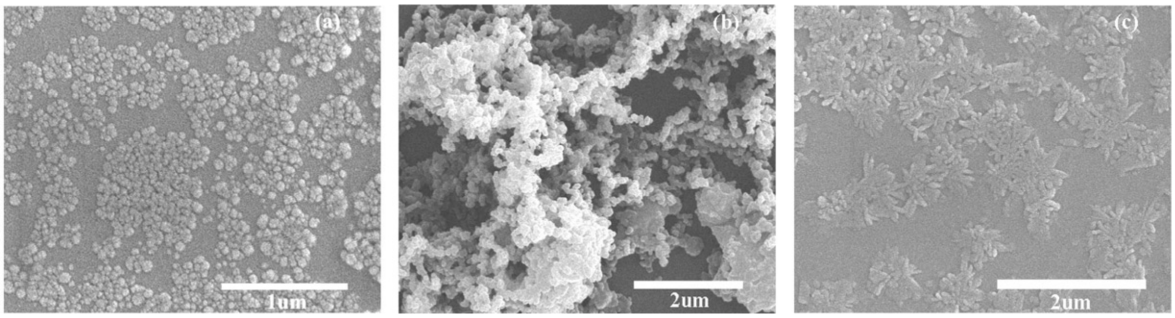

Fig. 4 The morphology of $CaCO_3$ formed in an ODA/Ca^{2+} LB film after immersing into a 0.001 M Na_2CO_3 solution for (a) 2, (b) 5, (c) 600 min.

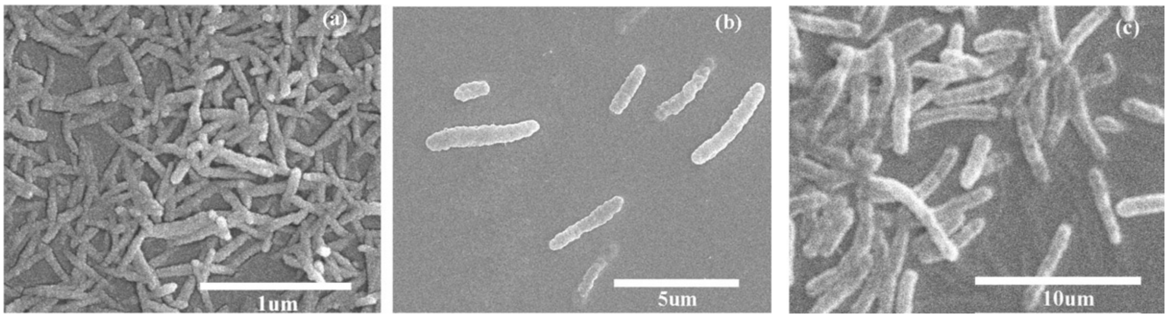

Fig. 5 The morphology of $CaCO_3$ formed in an ODA/Ca^{2+} LB film after immersing into a 0.1 M Na_2CO_3 solution for (a) 2, (b) 5, (c) 600 min.

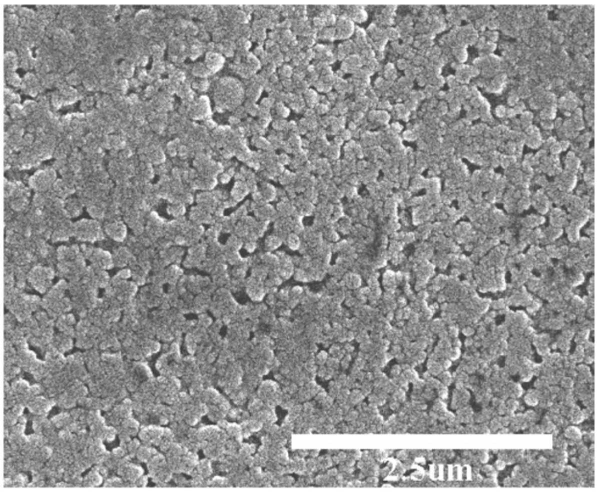

Fig. 6 The morphology of $CaCO_3$ when the stearic acid/Ca^{2+} LB film is immersed into a 0.01 M Na_2CO_3 solution for 2 min.

surface when forming metal complexes with divalent transition metal ions.[20,21,27] In the case of salt formation with Ca^{2+}, a similar structure b, shown in Scheme 1, is proposed with the two heads of the ODA molecules being connected by the metal ions. Such a conformation could be kept when transferring onto the solid substrates. When the template film is immersed into the Na_2CO_3 solution, $CaCO_3$ nanoparticles grow at the two ends of the ODA. With increasing the amount of $CaCO_3$, the nanoparticles aggregate through the ionic linkages and bundles, as shown in Scheme 1c and d. Because the interaction between Ca^{2+} and COO^- is not so strong as with transition metal ions, only short nanorods are formed. This is clearly verified by the time-dependent morphological changes of $CaCO_3$

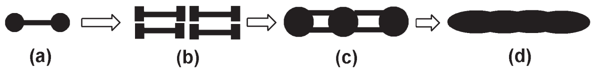

Scheme 1 Possible formation process of $CaCO_3$ nanorods in the LB film of ODA/Ca^{2+}: (a) bolaamphiphile, (b) ODA/Ca^{2+} Langmuir film, (c) growth of $CaCO_3$ particles at the two ends of the bolaamphiphile, (d) nanoparticles aggregate along the bundles of the alkyl chains to form the nanorods.

in the templated LB films. In addition, due to the fact that the Langmuir film at the air–water interface is not formed in one direction, the bolaamphiphile can extend in all directions; therefore, the nanorods in our case are not aligned.

Conclusion

1,18-Octadecanedicarboxylic acid, a bolaamphiphilic diacid, can form stable Langmuir films with Ca^{2+} at the air–water interface. The Langmuir film can be transferred onto solid substrates by using the LB technique. The film can be used as a template to grow $CaCO_3$. It was found that nanoparticles were obtained at the shortest times. At longer immersion times and in concentrated Na_2CO_3 solution, nanorods and aggregates of nanorods were observed. It is suggested the structure of the bolaamphiphile plays an important role in the formation of such nanorods. The nanoparticles are suggested to aggregate through the ionic grooves of the bolaamphiphilic template structure.

Acknowledgements

This work was supported by the Outstanding Youth Fund (no. 20025312), the Major State Basic Research Development Program (G2000078103), and the Fund of the Chinese Academy of Sciences.

References

1 M. Antonietti and C. Göltner, *Angew. Chem., Int. Ed. Engl.*, 1997, **36**, 910.
2 J. P. Spatz, A. Roescher and M. Möller, *Adv. Mater.*, 1996, **8**, 337.
3 M. Moffit and A. Eisenberg, *Chem. Mater.*, 1995, **7**, 1178.
4 G. Schmid, *Chem. Rev.*, 1992, **92**, 1709.
5 L. T. Chang and C. C. Yen, *J. Appl. Polym. Sci.*, 1995, **55**, 371.
6 F. Mafuné, J. Kohno, Y. Takeda and T. Kondow, *J. Phys Chem. B*, 2000, **104**, 9111.
7 L. Qi, J. Ma, H. Cheng and Z. Zhao, *J. Phys. Chem. B*, 1997, **101**, 3460.
8 D. Zhang, L. Qi, J. Ma and H. Cheng, *Chem. Mater.*, 2001, **13**, 2753.
9 L. Qi, H. Cölfen and M. Antonietti, *Angew. Chem., Int. Ed.*, 2000, **39**, 604.
10 L. Qi, H. Cölfen and M. Antonietti, *Chem. Mater.*, 2000, **12**, 2392.
11 H. Zhao, E. P. Douglas, B. S. Harrison and K. S. Schanze, *Langmuir*, 2001, **17**, 8428.
12 X. Jiang, Y. Xie, J. Lu, L. Zhu, W. He and Y. Qian, *J. Mater. Chem.*, 2001, **11**, 1775.
13 S. Guo, L. Konopny, R. Popovitz-Biro, H. Cohen, H. Porteanu, E. Lifshitz and M. Lahav, *J. Am. Chem. Soc.*, 1999, **121**, 9589.
14 C. C. Chen and J. J. Lin, *Adv. Mater.*, 2001, **13**, 136.
15 Y. J. Han, J. M. Kim and G. D. Stucky, *Chem. Mater.*, 2000, **12**, 2068.
16 A. Govindaraj, B. C. Satishkumar, M. Nath and C. N. R. Rao, *Chem. Mater.*, 2000, **12**, 202.
17 E. S. Smotkin, C. Lee, A. J. Bard, A. Campion, M. A. Fox, T. E. Mallouk, S. E. Webber and J. M. White, *Chem. Phys. Lett.*, 1988, **152**, 265.
18 B. O. Dabbousi, C. B. Murray, M. F. Rubner and M. G. Bawendi, *Chem. Mater.*, 1994, **6**, 216.
19 B. Li, Y. Liu, J. Yu, Y. Bai, W. Pang and R. Xu, *Langmuir*, 1999, **15**, 4837.
20 S. Guo, R. Popovitz-Biro, T. Arad, G. Hodes, L. Leiserowitz and M. Lahav, *Adv. Mater.*, 1998, **10**, 657.
21 S. Guo, R. Popovitz-Biro, I. Weissbuch, H. Cohen, G. Hodes and M. Lahav, *Adv. Mater.*, 1998, **10**, 121.
22 V. Hensel, A. Godt, R. Popovitz-Biro, H. Cohen, T. R. Jensen, K. Kjaer, I. Weissbuch, E. Lifhitz and M. Lahav, *Chem.-Eur. J.*, 2002, **8**, 1413.
23 H. Fuhrhop and D. Fritsch, *Acc. Chem. Res.*, 1986, **19**, 130.
24 H. Fuhrhop and J. Matthieu, *Angew. Chem., Int. Ed. Engl.*, 1984, **23**, 100.
25 G. H. Escamilla and G. R. Newkome, *Angew. Chem., Int. Ed. Engl.*, 1994, **33**, 1937.
26 Q. Lu, Y. H. Luo, L. Li and M. H. Liu, *Langmuir*, 2003, **19**, 285.
27 I. Weissbuch, S. Guo, R. Edgar, S. Cohen, P. Howes, K. Kjaer, M. Lahav and L. Leiserowitz, *Adv. Mater.*, 1998, **10**, 117.
28 I. Kuzmenko, H. Rapaport, K. Kjaer, J. Als-Nielsen, I. Weissbuch, M. Lahav and L. Leiserowitz, *Chem. Rev.*, 2001, **101**, 1659.
29 M. Sedlak, M. Antonietti and H. Cölfen, *Macromol. Chem. Phys.*, 1998, **199**, 247.
30 H. Cölfen and M. Antonietti, *Langmuir.*, 1998, **14**, 582.
31 J. M. Marentette, J. Norwig, E. Stockelmann, W. H. Meyer and G. Wegner, *Adv. Mater.*, 1997, **9**, 647.
32 D. D. Archibald, S. B. Qadri and B. P. Gaber, *Langmuir*, 1996, **12**, 538.
33 J. Aizenberg, A. J. Black and G. M. Whitesides, *Nature (London)*, 1999, **398**, 495.